

Crystal Structures of Complexes of *N*-Butyl- and *N*-Nonyl-Deoxyojirimycin Bound to Acid β -Glucosidase

INSIGHTS INTO THE MECHANISM OF CHEMICAL CHAPERONE ACTION IN GAUCHER DISEASE*

Received for publication, June 18, 2007, and in revised form, July 30, 2007. Published, JBC Papers in Press, July 31, 2007, DOI 10.1074/jbc.M705005200

Boris Brumshtein[‡], Harry M. Greenblatt[‡], Terry D. Butters[§], Yoseph Shaaltiel[¶], David Aviezer[¶], Israel Silman^{||}, Anthony H. Futerman^{**1}, and Joel L. Sussman^{‡2}

From the Departments of [‡]Structural Biology, ^{||}Neurobiology, and ^{**}Biological Chemistry, Weizmann Institute of Science, Rehovot 76100, Israel, [§]Glycobiology Institute, Department of Biochemistry, University of Oxford, South Parks Road, Oxford OX1 3QU, United Kingdom, and [¶]Protalix Biotherapeutics, 2 Snunit Street, Science Park, Carmiel 20100, Israel

Gaucher disease is caused by mutations in the gene encoding acid β -glucosidase (GlcCerase), resulting in glucosylceramide (GlcCer) accumulation. The only currently available orally administered treatment for Gaucher disease is *N*-butyl-deoxyojirimycin (ZavescaTM, NB-DNJ), which partially inhibits GlcCer synthesis, thus reducing levels of GlcCer accumulation. NB-DNJ also acts as a chemical chaperone for GlcCerase, although at a different concentration than that required to completely inhibit GlcCer synthesis. We now report the crystal structures, at 2 Å resolution, of complexes of NB-DNJ and *N*-nonyl-deoxyojirimycin (NN-DNJ) with recombinant human GlcCerase, expressed in cultured plant cells. Both inhibitors bind at the active site of GlcCerase, with the imino sugar moiety making hydrogen bonds to side chains of active site residues. The alkyl chains of NB-DNJ and NN-DNJ are oriented toward the entrance of the active site where they undergo hydrophobic interactions. Based on these structures, we make a number of predictions concerning (i) involvement of loops adjacent to the active site in the catalytic process, (ii) the nature of nucleophilic attack by Glu-340, and (iii) the role of a conserved water molecule located in a solvent cavity adjacent to the active site. Together, these results have significance for understanding the mechanism of action of GlcCerase and the mode of GlcCerase chaperoning by imino sugars.

Mutations in the gene encoding acid β -glucosidase (GlcCerase³, E.C. 3.2.1.45) cause Gaucher disease, the most common lysosomal storage disorder (1–5). GlcCerase hydrolyzes the β -glycosidic bond of glucosylceramide (GlcCer) to yield glucose and ceramide (6). Solution of the x-ray structure of GlcCerase demonstrated that it contains three non-contiguous domains (7). Domain I consists of a major 3-stranded anti-parallel β -sheet flanked by a perpendicular N-terminal strand and loop. Domain II consists of two closely associated β -sheets forming an independent domain resembling an immunoglobulin fold. Domain III is a $(\beta/\alpha)_8$ (TIM) barrel containing the catalytic site (7).

Subsequent structural studies led to increased understanding of the GlcCerase structure (8) and to solution of GlcCerase structures (Table 1) to which small molecules were bound, either covalently, *i.e.* conduritol-B-epoxide (1,2-anhydro-*myo*-inositol; CBE) (5), or non-covalently, *i.e.* isofagomine (IFG) (9) (Fig. 1). No structures of mutant enzymes are yet available, but recent work has demonstrated that some mutants cause a loss of protein stability during biosynthesis, whereas other mutants result in loss of catalytic activity (10, 11).

At present, two treatments are available for Gaucher disease patients. The first is enzyme replacement therapy using recombinant human GlcCerase (CerezymeTM) expressed in Chinese hamster ovary cells (12–14). The second is substrate reduction therapy, in which partial inhibition of glycosphingolipid synthesis by *N*-butyl-deoxyojirimycin (NB-DNJ; ZavescaTM) (15) decreases accumulation of glycosphingolipids, including GlcCer. A third therapeutic option is on the horizon, namely chaperone therapy, in which active site-directed inhibitors are used to stabilize mutant forms of GlcCerase as they pass through the secretory pathway (16, 17). Interestingly, NB-DNJ and *N*-nonyl-deoxyojirimycin (NN-DNJ) also act as chemical chaperones of GlcCerase (18), since elevated GlcCerase activity occurs upon incubation of cultured cells expressing various GlcCerase mutants with NN-DNJ or NB-DNJ (19, 20). Thus, NB-DNJ and NN-DNJ inhibit both GlcCer synthase (15) and

* This work was supported in part by the Magnetron Program, Office of the Chief Scientist, Ministry of Industry and Commerce, Israel, the Nalvyco Foundation, the Bruce Rosen Foundation, the William Singer Foundation, the Jean and Julia Goldwurm Memorial Foundation, the Kimmelman Center for Biomolecular Structure and Assembly, the Benziyo Center for Neuroscience, an Israel Ministry of Science, Culture, and Sport grant for the Israel Structural Proteomics Center, the Divadol Foundation, the Neuman Foundation, the Israel Science Foundation, and the European Commission Sixth Framework Research and Technological Development Programme "SPINE2-COMPLEXES" Project under contract 03122. The costs of publication of this article were defrayed in part by the payment of page charges. This article must therefore be hereby marked "advertisement" in accordance with 18 U.S.C. Section 1734 solely to indicate this fact.

The atomic coordinates and structure factors (code 2v3d, 2v3e) have been deposited in the Protein Data Bank, Research Collaboratory for Structural Bioinformatics, Rutgers University, New Brunswick, NJ (<http://www.rcsb.org/>).

¹ Joseph Meyerhoff Professor of Biochemistry at the Weizmann Institute of Science. To whom correspondence should be addressed. Tel.: 972-8-9342704; Fax: 972-8-9344112; E-mail: tony.futerman@weizmann.ac.il.

² Morton and Gladys Pickman Professor of Structural Biology at the Weizmann Institute.

³ The abbreviations used are: GlcCerase, acid β -glucosidase; CBE, conduritol-B-epoxide; endo-GCase II, endo-glycoceramidase II; GlcCer, glucosylceramide; IFG, isofagomine; NB-DNJ, *N*-butyl-deoxyojirimycin; NN-DNJ, *N*-nonyl-deoxyojirimycin; GM3, NeuAc α 2,3Gal β 1,4Glc-ceramide; DG, deglycosylated.

GlcCerase, although at different concentrations (18, 19). The mechanism of inhibition, or of binding to GlcCerase, is not known.

We now report the crystal structures of complexes of NB-DNJ and NN-DNJ with recombinant human GlcCerase, expressed in cultured plant cells (pGlcCerase) (21); the structure of pGlcCerase is highly homologous to that of CerezymeTM (21). We compare the structures of pGlcCerase complexed to NB-DNJ and NN-DNJ with that of a complex of CerezymeTM with another potential chaperone, IFG, and demonstrate some important differences in their mode of binding that have implications for understanding the catalytic cycle of GlcCerase and the mode of its chaperoning by imino sugars.

EXPERIMENTAL PROCEDURES

Crystallization—pGlcCerase was produced as described (21). The enzyme was diluted in crystallization buffer (0.02%

NaN₃/10 mM sodium citrate, pH 5.5, containing 7% (v/v) ethanol, washed three times, and concentrated to 4–5 mg/ml in a Centricon[®] device using a filter with a 30-kDa cut-off. NB-DNJ and NN-DNJ were dissolved in water to yield 0.1-M stock solutions and added to the pGlcCerase solution to a final concentration of 13 mM. CocrySTALLIZATION was performed using the micro-batch technique under oil. Protein and crystallization solutions were dispensed into micro-batch crystallization plates under oil (1:1 v/v silicone and paraffin oils), such that the final solution contained 50% protein solution and 50% crystallization liquor. The best diffracting crystals of NB-DNJ/pGlcCerase were obtained in 0.2 M (NH₄)₂SO₄/0.1 M Tris, pH 6.5, 25% (w/v) polyethylene glycol 3350, and the best crystals of NN-DNJ/pGlcCerase were obtained using 0.2 M NH₄COOCH₃/0.1 M Hepes, pH 7.5, 25% (w/v) polyethylene glycol 3350. Crystals were cryo-protected with 20% (v/v) ethylene glycol for x-ray data collection.

Data Collection and Refinement

Data were collected on the BM14 beamline of the European Synchrotron Radiation Facility (Grenoble, France). Images were indexed with the HKL2000 software package and scaled with SCALEPACK (22). The structures of NB-DNJ/pGlcCerase and NN-DNJ/pGlcCerase were solved using rigid body refinement and refined with Refmac5 (23) (Table 2). The crystal structure of pGlcCerase (21) (PDB code 2v3f) was used as a starting model, and FreeR flags were taken from the corresponding structure factors file. Model manipulation and water editing was performed using Coot graphics software (24). Images were created with PyMol and LIGPLOT (25). Structures and structure factors were deposited in the Protein Data Bank (code 2v3d for NB-DNJ/pGlcCerase and code 2v3e for NN-DNJ/pGlcCerase-NN-DNJ) (Table 1).

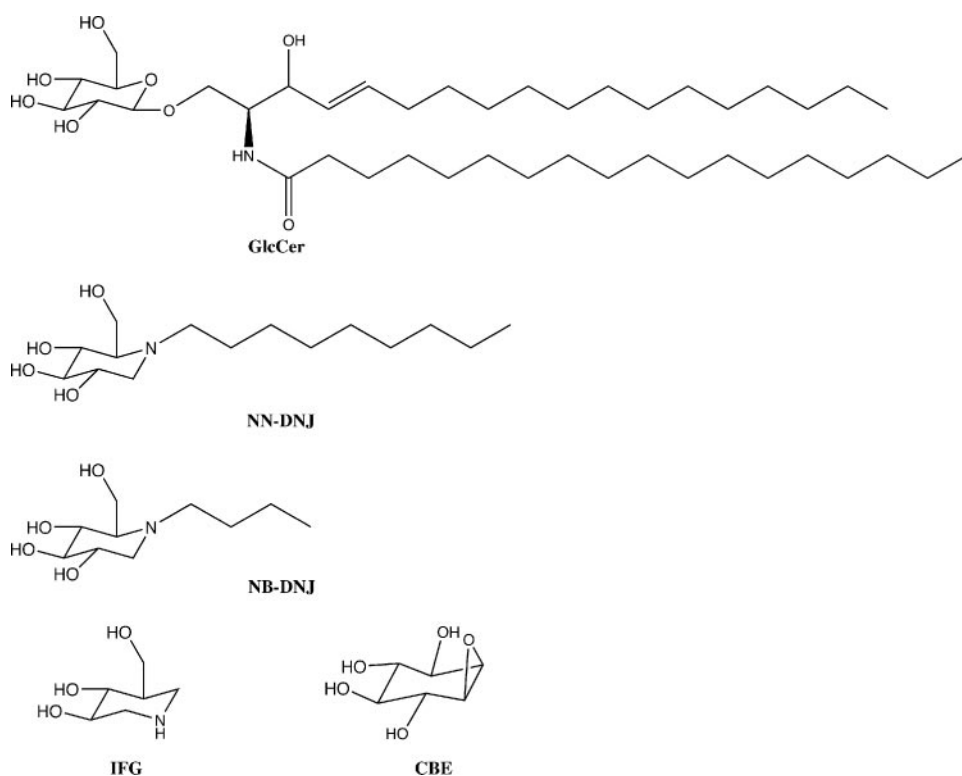


FIGURE 1. Structures of lipids and inhibitors discussed in this study.

TABLE 1

GlcCerase structures solved to date, and the abbreviations used in the current study

Enzyme source	Treatment prior to crystallization	Bound molecule	PDB code	Reference	Abbreviation
Cerezyme TM ^a	Partial deglycosylation ^b	None	1ogs	(7)	DG-Cerezyme
Cerezyme TM	Partial deglycosylation	CBE	1y7v	(5)	CBE-DG-Cerezyme
Cerezyme TM	Partial deglycosylation	None	2f61	(28)	DG-Cerezyme
Cerezyme TM	None	None	2j25	(8)	Cerezyme
Cerezyme TM	Partial deglycosylation	IFG	2nsx	(9)	IFG/DG-Cerezyme
Cerezyme TM	Partial deglycosylation	Glycerol	2nt0	(9)	Glyc/DG-Cerezyme
Cerezyme TM	Partial deglycosylation	None	2nt1	(9)	DG-Cerezyme
Human GlcCerase expressed in plant cells ^c	None	None	2v3f	(21)	pGlcCerase
Human GlcCerase expressed in plant cells	None	NB-DNJ	2v3d	Current study	NB-DNJ/pGlcCerase
Human GlcCerase expressed in plant cells	None	NN-DNJ	2v3e	Current study	NN-DNJ/pGlcCerase

^a Recombinant human enzyme expressed in Chinese hamster ovary cells.

^b For details, see Ref. 7.

^c Ref. 21.

Structure of Acid β -Glucosidase Bound to Imino Sugars

TABLE 2

Data collection and refinement statistics

Highest resolution shell is shown in parentheses.

	NB-DNJ/pGlcCerase	NN-DNJ/pGlcCerase
Data collection		
Space group	P2 ₁	P2 ₁
Cell dimensions		
<i>a</i> , <i>b</i> , <i>c</i> (Å)	67.99, 97.21, 82.40	67.99, 97.64, 82.35
β (°)	102.91	102.75
Resolution (Å)	50.00-1.96 (2.03-1.96)	50.00-2.00 (2.07-2.00)
<i>R</i> _{sym} (%)	7.4 (42.1)	8.1 (34.3)
<i>I</i> / σ (<i>I</i>)	16.6 (2.6)	10.27 (2.1)
Completeness (%)	96.8 (91.8)	88.9 (52.2)
Redundancy	3.7 (3.4)	2.0 (2.0)
Refinement		
Resolution (Å)	25.22-1.96	23.62-2.00
Number of reflections	68290	59655
<i>R</i> _{work} / <i>R</i> _{free}	15.3/20.8	16.2/22.0
Root mean square deviations		
Bond lengths (Å)	0.016	0.016
Ramachandran outliers (%)	0.2	0.2
Bond angles (°)	1.484	1.550
Number of refined atoms		
Protein	7864	7861
Carbohydrates	112	112
Solvent	1002	1014
Ligands	30	40

Modeling of Michaelis-Menten Complexes—The imino sugar of NN-DNJ was used to build a model of GlcCer in the pGlcCerase active site. Because the aliphatic chain of NN-DNJ does not resemble the sphingoid base or the *N*-acylated fatty acid of GlcCer, the ceramide moiety was modeled on the basis of the crystal structure of the complex of ganglioside GM3 with endo-glycoceramidase II (endo-GCase II) (PDB 2OSX) (26). The catalytic residues of endo-GCase II were aligned with those of GlcCerase (with Glu-233 of endo-GCase II corresponding to Glu-235 of GlcCerase, and Ser-351 of endo-GCase II corresponding to Glu-340 of GlcCerase; in addition, His-304 of endo-GCase II was aligned with His-311 of GlcCerase). The glucose moiety of GlcCer did not exactly overlay the imino sugar of either NN- or NB-DNJ; therefore, the structure of GlcCer was modeled using the torsion angles of the GlcCer moiety of GM3 bound to endo-GCase II. In addition, the torsion angles of the glucoside bond and of some bonds of the *N*-acyl chain were modified to avoid steric clashes.

RESULTS AND DISCUSSION

Binding of NB-DNJ and NN-DNJ to the Active Site of pGlcCerase—Crystals of NB-DNJ/pGlcCerase and NN-DNJ/pGlcCerase were obtained in space group P2₁ (Table 2), with two protein molecules in the asymmetric unit. Superimposition of the native pGlcCerase structure (21) on those of NB-DNJ/pGlcCerase or NN-DNJ/pGlcCerase resulted in root mean square deviations of only 0.2 and 0.3 Å, respectively, showing that neither of these ligands produces a global structural change upon binding to the enzyme.

Both inhibitors bind to the active site of pGlcCerase, with the imino sugar making hydrogen bonds with side chains of active site residues (Figs. 2 and 3). Hydrogen bond distances between the imino sugar and the active site residues are similar for NB-DNJ and NN-DNJ. The alkyl chains of NB-DNJ and NN-DNJ

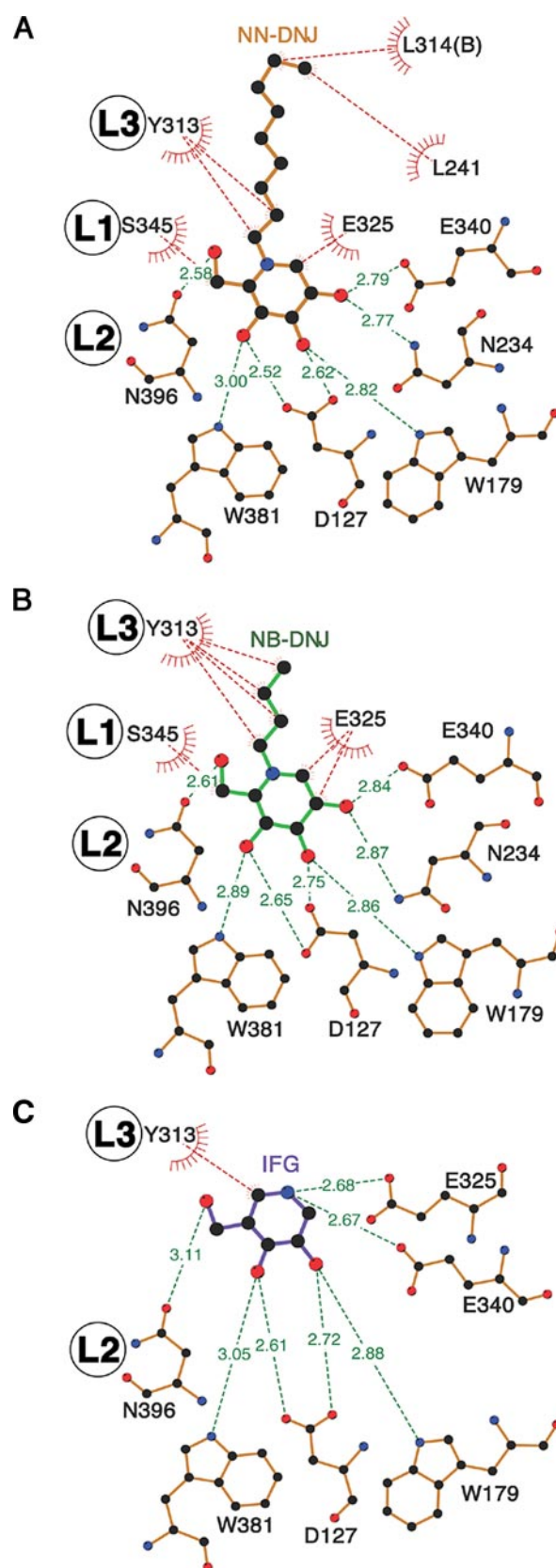


FIGURE 2. Comparison of binding of non-covalent inhibitors to GlcCer. A, NN-DNJ/pGlcCerase. B, NB-DNJ/pGlcCerase. C, IFG/DG-Cerezyme. Green lines represent hydrogen bonds and red lines hydrophobic interactions. L1, loop 1 (residues 341–350); L2, loop 2 (residues 393–396); L3, loop 3 (residues 312–319). 314(B) in panel A corresponds to the side chain of a symmetrically related molecule.

are oriented toward the entrance of the active site. The interactions of pGlcCerase with these alkyl chains are via hydrophobic interactions and are, therefore, less specific than the hydrogen bond interactions formed with the pyranose ring, consistent with the ability of imino sugars with alkyl chains of varying lengths to bind to GlcCerase (18). The alkyl chains of both inhibitors are stabilized by interaction with Tyr-313 near the active site, and the alkyl chain of NN-DNJ makes an additional contact with Leu-314, near the entrance to the active site (Fig. 2A). Interestingly, there is a >300-fold difference in the K_i values of the two inhibitors (116 μM for NB-DNJ and 0.3 μM for NN-DNJ) (27), which cannot be accounted for by this one additional contact. Rather, the lower K_i of NN-DNJ is most likely a reflection of the increased overall hydrophobicity of NN-DNJ compared with NB-DNJ (Table 3), with the hydrophobic surface at the entrance to the active site favoring the more hydrophobic ligand.

Comparison of the structures of NB-DNJ/pGlcCerase and NN-DNJ/pGlcCerase with that of IFG/DG-Cerezyme (9) demonstrates that the pyranose-like ring makes a similar number of hydrogen bonds with the enzyme in all three cases (Fig. 2 and Table 3). Where these structures differ significantly is in the interaction of their nitrogen atoms with the active site of GlcCerase. The secondary amine in IFG is structurally homologous to the anomeric carbon of GlcCer and is located between the two catalytic glutamic acid residues, Glu-325 and Glu-340, forming hydrogen bonds with each of their carboxyl moieties. In contrast, the tertiary amines of NN-DNJ and NB-DNJ are located in a position similar to that of the ring oxygen of GlcCer and do not, therefore, form any hydrogen bonds or salt bridges with GlcCerase.

Loops at the Entrance to the Active Site—The active site of GlcCerase is formed on one side by three loops, which have

been observed in a number of conformations (Figs. 3 and 4) (5, 7, 8, 28). However, in all GlcCerase structures to which an inhibitor was bound, only one set of conformations was observed (5, 9), which was the same as that observed in pGlcCerase crystallized in a $P2_1$ space group (21). The conformation of the active site-associated loops presumably facilitates substrate binding. Thus, the side chain of Asn-396 on loop 2 forms a hydrogen bond with the inhibitor hydroxyl group that corresponds to the same group on the non-chiral pyranose carbon atom of GlcCer (Fig. 2). Loop 3 shows even more flexibility, in some cases adopting a helical structure, whereas in others it assumes a coil.

One residue on loop 3 that appears relevant to catalysis is Tyr-313. In the three structures to which a non-covalent inhibitor is bound (NB-DNJ/pGlcCerase, NN-DNJ/pGlcCerase, and IFG/DG-Cerezyme), the hydroxyl group of Tyr-313 hydrogen bonds to Glu-340. This requires loop 3 to be in a helical conformation. In the structure with a covalent inhibitor (CBE-DG-Cerezyme), in which CBE is covalently attached to Glu-340, Tyr-313Oⁿ forms a hydrogen bond with Glu-235 and loop 3 assumes a coil conformation. If the two observed interactions of Tyr-313 are adopted by the enzyme during catalysis, then a conformational change in loop 3 may be an integral element of the GlcCerase reaction mechanism.

Loop 1 does not display major changes in its backbone angles or in its secondary structure. However, it appears to be affected by crystal contacts (8), and hence some movements in this loop are observed. Specifically, the aromatic residues on loop 1, Trp-348 and Phe-347, are involved in crystal contacts, and it is therefore possible that it is more mobile in solution. The mobility of these hydrophobic residues may be relevant to the association of GlcCerase with the lipid membrane (8).

Catalytic Mechanism of GlcCerase—Based on the structures reported herein, and on that of GM3 bound to the active site of endo-GCase II (26), we modeled GlcCer in the active site of GlcCerase (Fig. 5), allowing us to examine the reaction mechanism of GlcCerase. Three issues arose out of this analysis.

First, while there is significant evidence to support a nucleophilic role for Glu-340 in the GlcCerase catalytic cycle, several recent studies (e.g. Ref. 29) have implied direct attack of the carboxylate oxygen of Glu-340 on the anomeric carbon of GlcCer. The NN-DNJ/pGlcCerase and NN-DNJ/pGlcCerase struc-

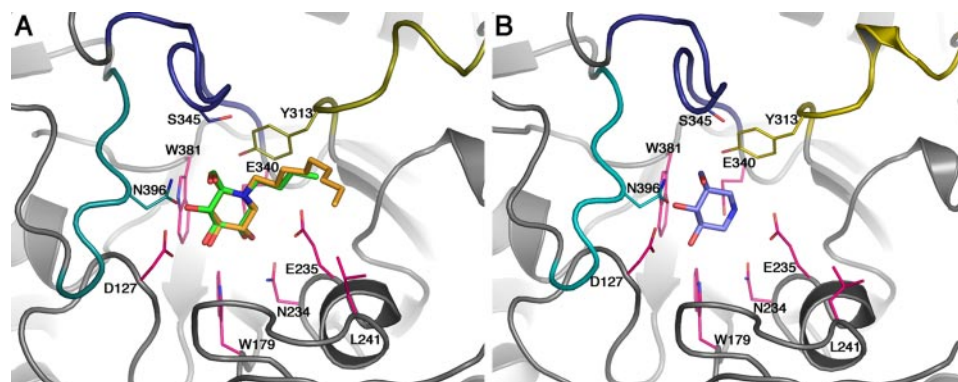


FIGURE 3. **Binding of inhibitors to the active site of GlcCerase.** A, NB-DNJ and NN-DNJ bound to pGlcCerase. B, IFG bound to DG-Cerezyme (9). Side chains of the residues involved in binding are shown as sticks; loop 3 is shown in yellow, loop 1 in blue, and loop 2 in teal.

TABLE 3
Number and type of bonds in structures of GlcCerase complexes

Side chains of residues with van der Waals distances $\leq 4 \text{ \AA}$ to the ligand were considered as non-polar contacts.

Structure	Number of H-bonds	Number of residues with Van der Waals contacts	CLogP ^a	pK _a of nitrogen
IFG/DG-Cerezyme	7	1	-2.0	
NB-DNJ/pGlcCerase	7	3	0.9	7.1
NN-DNJ/pGlcCerase	7	4 (5) ^b	3.5	6.7

^a Calculation of hydrophobicity (cLogP) was performed for each molecule in its reduced state, using ChemDraw 7.0.1 software.

^b Parentheses indicate a contact to a symmetry-related molecule.

Structure of Acid β -Glucosidase Bound to Imino Sugars

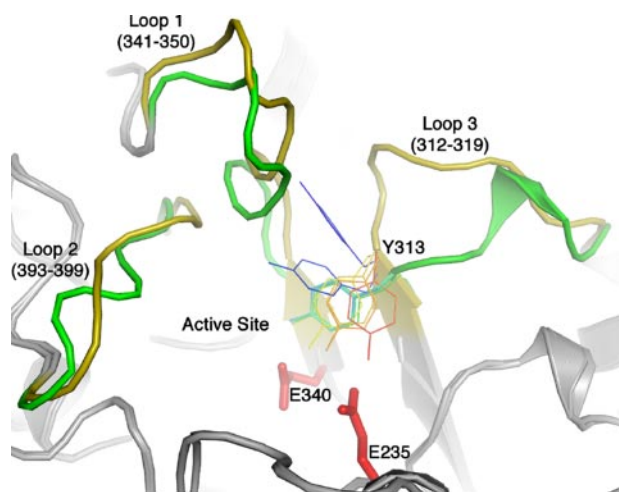


FIGURE 4. Conformations of the loops at the entrance to the active site. The loops in GlcCerase occur in a number of conformations, but only two are shown for clarity, in yellow and green; these conformations give the most pronounced changes in the entrance to the active site. Tyr-313, which may play a role in the catalytic mechanism, is indicated. The catalytic residues are shown as red sticks.

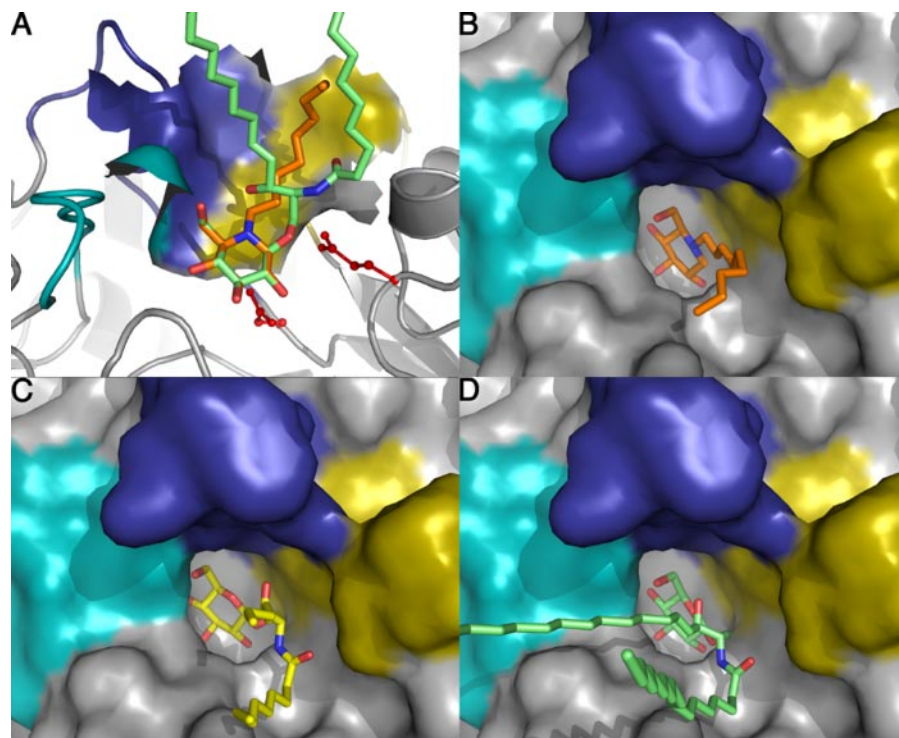


FIGURE 5. Comparison of binding of inhibitors to GlcCerase with binding of GlcCer to GlcCerase. *A*, a model of GlcCer (green) is overlaid on the experimental structure of NN-DNJ (orange). Loops enclosing the active site are shown in blue (loop 1), teal (loop 2), and yellow (loop 3). Catalytic residues are shown as red sticks and spheres. *B*, NN-DNJ (orange) in the active site of GlcCerase. *C*, structure of the GlcCer moiety (yellow sticks) of GM3 from endo-GCase II aligned into the active site of GlcCerase. *D*, model of GlcCer in the active site of GlcCerase.

tures do not support such a direct attack, because the apical hydrogen on the anomeric carbon is positioned between the carbon atom and the attacking oxygen atom in such a way that it would block nucleophilic attack by steric hindrance (Fig. 6). If, however, there is an intermediate involving a planar carbon atom, attack by Glu-340 would be possible (30, 31). In the case of CBE, direct nucleophilic attack on the epoxide carbon by

Glu-340 is possible, because the hydrogen atom is not apical, rendering the carbon susceptible to such attack.

The second issue concerns the protonation state of Glu-235. This residue corresponds to Glu-35 in lysozyme, which supplies a proton to the leaving group in the initial stage of the reaction and thus must be protonated in the resting state of the enzyme (30, 31). The basic limb of the pH/activity profile of lysozyme, with a pK_a of ~ 6.5 , is attributed to deprotonation of Glu-35. The elevated pK_a of this residue in lysozyme has been explained by it being partially buried. GlcCerase has a similar pH/activity profile, with pK_a s of 4.5 and 6.5 (32, 33). However, in Cerezyme (8), Glu-235 is near His-311 $N^{\delta 1}$ (3.2 Å), Asn-234 (3.3 Å), and Gln-284 (3.6 Å). His-311 is part of a hydrogen bond network involving Asp-282, Arg-120, and the catalytic residue Glu-340 (Fig. 7). Given its proximity to Asp-282, it is presumably protonated, despite being buried in the active site. The close proximity of polar residues, particularly if His-311 is charged, should only serve to lower the pK_a of Glu-235 rather than raising it to pH 6.5. Further investigation is thus required to understand the protonation states of these residues.

The third issue concerns the role of water in the catalytic mechanism; a water molecule is required for hydrolysis of the covalent intermediate. In all GlcCerase structures of sufficient resolution to see water molecules (1OGS, 1Y7V, 2NSX, 2NT0, 2NT1, 2V3F, 2V3D, and 2V3E), a cavity near the catalytic residue Glu-235 contains water molecules. One particular water molecule at an equivalent location is visible in other glycosidase structures, such as endo-GCase II (26) and xylanase (34). These conserved water molecules may be involved in the catalytic cycle because the solvent cavity is located next to the catalytic residues and is accessible from the active site (Fig. 8).⁴

CONCLUSIONS

NB-DNJ is the only currently available orally administered drug for treatment of Gaucher disease. Its primary effect is via inhibition of GlcCer synthase; however, the compound also has a coincidental chaperone effect on GlcCerase. The chaperoning effect of NN-DNJ was

⁴ A fourth issue can also be considered, namely an anion binding site. During refinement of the structure of NN-DNJ/pGlcCerase, we detected a phosphate ion coordinated by the side chains of Ser-12, Arg-353, and Ser-356. Because neither phosphate nor sulfate ions were added to the crystallization solutions, it is possible that the phosphate ion was co-purified with the enzyme (21). This location is occupied either by a phosphate or a sulfate ion in all the previously published GlcCerase structures and may implicate this site as a possible binding site upon association of GlcCerase with the lipid bilayer (8).

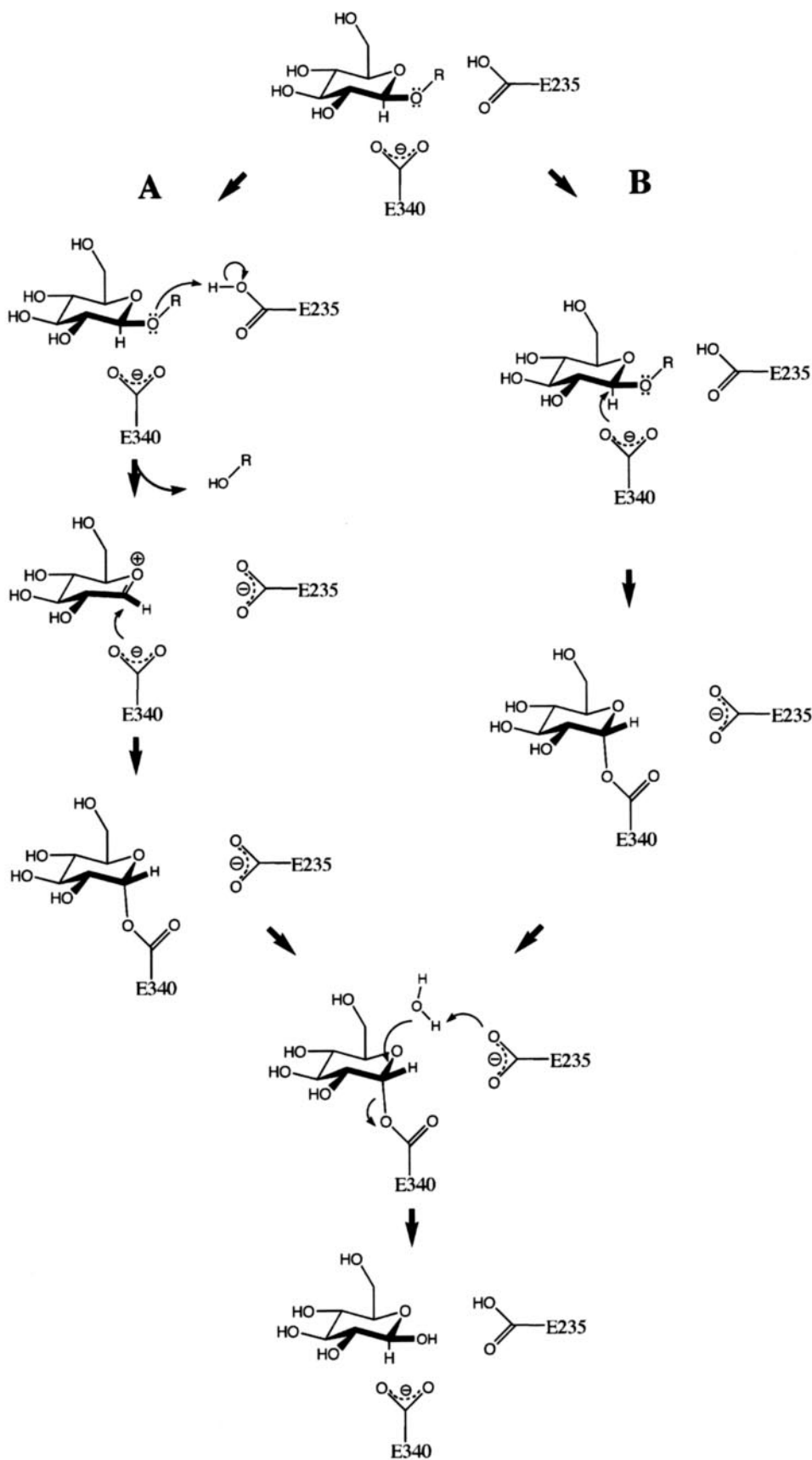


FIGURE 6. **Proposed modified catalytic mechanism of GlcCerase.** In *scheme A*, the anomeric carbon of glucose would not be susceptible to nucleophilic attack by Glu-340 due to steric clashes with the hydrogen atom of the glucose anomeric carbon. Hydrolysis of the glycoside bond must, therefore, proceed through a carbenium ion intermediate. *B*, the commonly accepted mechanism assumes a direct nucleophilic attack on the anomeric carbon, without formation of a carbenium ion intermediate.

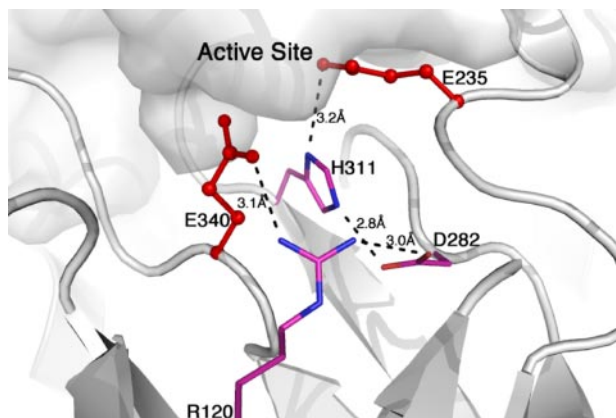


FIGURE 7. A hydrogen bond network around His-311 and Glu-235. Residues Arg-120, Asp-282, His-311, and Glu-340 are presumably charged. The presence of the charged imidazole moiety of His-311 is likely to lower the pK_a of Glu-235.

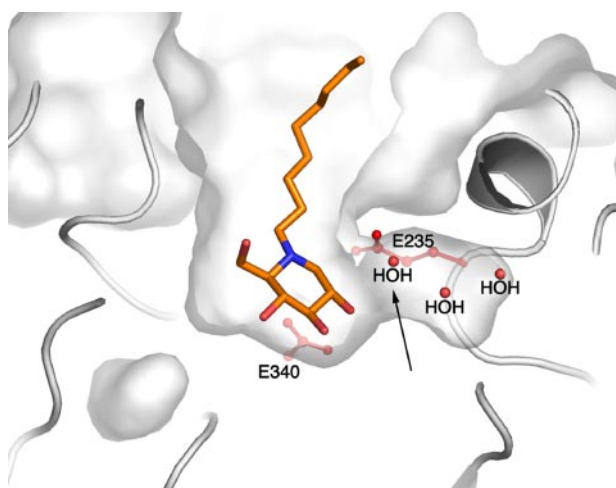


FIGURE 8. A solvent pocket adjacent to catalytic Glu-235. The water molecule common to other glycosidase structures is identified by an arrow.

shown to be specific for GlcCerase with mutations in the catalytic domain, domain III (11, 19, 35). The crystal structures of NB-DNJ/pGlcCerase and NN-DNJ/pGlcCerase reported herein are consistent with these observations, because the inhibitor binds at the active site. The pK_a of NB-DNJ also appears to be advantageous for fulfilling its role as a chaperone. In the endoplasmic reticulum, where the protein is synthesized, the neutral pH is close to the pK_a of NB-DNJ. Under these conditions, NB-DNJ would be neutral (Table 3), and so less soluble, favoring binding to the active site. However, at the acidic pH of the lysosome, NB-DNJ would be charged, thus increasing its solubility and lowering the free energy of binding, thus competing less with GlcCer.

Acknowledgment—We thank Dr. M. Mackeen, Oxford Glycobiology Institute, for imino sugar pK_a determinations.

REFERENCES

1. Futerman, A. H., and Zimran, A. (2006) *Gaucher Disease*, Taylor and Francis Group, Boca Raton, FL

2. Futerman, A. H., and van Meer, G. (2004) *Nat. Rev. Mol. Cell Biol.* **5**, 554–565
3. Beutler, E., and Grabowski, G. A. (2001) in *The Metabolic and Molecular Bases of Inherited Disease* (Scriver, C. R., Sly, W. S., Childs, B., Beaudet, A. L., Valle, D., Kinzler, K. W., and Vogelstein, B., eds) 8th Ed., pp. 3635–3668, McGraw-Hill Inc., New York
4. Jmoudiak, M., and Futerman, A. H. (2005) *Br. J. Haematol.* **129**, 178–188
5. Premkumar, L., Sawkar, A. R., Boldin-Adamsky, S., Tokar, L., Silman, I., Kelly, J. W., Futerman, A. H., and Sussman, J. L. (2005) *J. Biol. Chem.* **280**, 23815–23819
6. Grabowski, G. A., Gatt, S., and Horowitz, M. (1990) *Critical Rev. Biochem. Mol. Biol.* **25**, 385–414
7. Dvir, H., Harel, M., McCarthy, A. A., Tokar, L., Silman, I., Futerman, A. H., and Sussman, J. L. (2003) *EMBO Rep.* **4**, 704–709
8. Brumshtein, B., Wormald, M. R., Silman, I., Futerman, A. H., and Sussman, J. L. (2006) *Acta Crystallogr. Sect. D Biol. Crystallogr.* **62**, 1458–1465
9. Lieberman, R. L., Wustman, B. A., Huertas, P., Powe, A. C., Jr., Pine, C. W., Khanna, R., Schlossmacher, M. G., Ringe, D., and Petsko, G. A. (2007) *Nat. Chem. Biol.* **3**, 101–107
10. Kolter, T., and Wendeler, M. (2003) *ChemBiochem.* **4**, 260–264
11. Sawkar, A. R., Schmitz, M., Zimmer, K. P., Reczek, D., Edmunds, T., Balch, W. E., and Kelly, J. W. (2006) *ACS Chem. Biol.* **1**, 235–251
12. Futerman, A. H., Sussman, J. L., Horowitz, M., Silman, I., and Zimran, A. (2004) *Trends Pharmacol. Sci.* **25**, 147–151
13. Brady, R. O. (1998) *Arch. Neurol.* **55**, 1055–1056
14. Desnick, R. J. (2004) *J. Inher. Metab. Dis.* **27**, 385–410
15. Platt, F. M., Neises, G. R., Dwek, R. A., and Butters, T. D. (1994) *J. Biol. Chem.* **269**, 8362–8365
16. Fan, J. Q. (2003) *Trends Pharmacol. Sci.* **24**, 355–360
17. Pastores, G. M., and Barnett, N. L. (2003) *Expert Opin. Investig. Drugs* **12**, 273–281
18. Butters, T. D., Dwek, R. A., and Platt, F. M. (2005) *Glycobiology* **15**, 43R–52R
19. Sawkar, A. R., Cheng, W. C., Beutler, E., Wong, C. H., Balch, W. E., and Kelly, J. W. (2002) *Proc. Natl. Acad. Sci. U. S. A.* **99**, 15428–15433
20. Alfonso, P., Pampin, S., Estrada, J., Rodriguez-Rey, J. C., Giraldo, P., Sanchó, J., and Pocovi, M. (2005) *Blood Cells Mol. Dis.* **35**, 268–276
21. Shaaltiel, Y., Bartfeld, D., Hashmueli, S., Baum, G., Brill-Almon, E., Galili, G., Dym, O., Boldin-Adamsky, S. A., Silman, I., Sussman, J. L., Futerman, A. H., and Aviezer, D. (2007) *Plant Biotech. J.* **5**, 579–590
22. Otwinowski, Z., and Minor, W. (1997) *Methods Enzymol.* **276**, 307–326
23. Murshudov, G. N., Vagin, A. A., and Dodson, E. J. (1997) *Acta Crystallogr. Sect. D Biol. Crystallogr.* **53**, 240–255
24. Emsley, P., and Cowtan, K. (2004) *Acta Crystallogr. Sect. D Biol. Crystallogr.* **60**, 2126–2132
25. Wallace, A. C., Laskowski, R. A., and Thornton, J. M. (1995) *Protein Eng.* **8**, 127–134
26. Caines, M. E., Vaughan, M. D., Tarling, C. A., Hancock, S. M., Warren, R. A., Withers, S. G., and Strynadka, N. C. (2007) *J. Biol. Chem.* **282**, 14300–14308
27. Yu, L., Ikeda, K., Kato, A., Adachi, I., Godin, G., Compain, P., Martin, O., and Asano, N. (2006) *Bioorg. Med. Chem.* **14**, 7736–7744
28. Liou, B., Kazimierczuk, A., Zhang, M., Scott, C. R., Hegde, R. S., and Grabowski, G. A. (2006) *J. Biol. Chem.* **281**, 4242–4253
29. Davies, G., and Henrissat, B. (1995) *Structure* **3**, 853–859
30. Legler, G. (1990) *Adv. Carbohydr. Chem. Biochem.* **48**, 319–384
31. Sinnott, M. L. (1990) *Chem. Rev.* **90**, 1171–1202
32. Erickson, J. S., and Radin, N. S. (1973) *J. Lipid Res.* **14**, 133–137
33. Osiecki-Newman, K., Legler, G., Grace, M., Dinur, T., Gatt, S., Desnick, R. J., and Grabowski, G. A. (1988) *Enzyme* **40**, 173–188
34. Larson, S. B., Day, J., Barba de la Rosa, A. P., Keen, N. T., and McPherson, A. (2003) *Biochemistry* **42**, 8411–8422
35. Sawkar, A. R., Adamski-Werner, S. L., Cheng, W. C., Wong, C. H., Beutler, E., Zimmer, K. P., and Kelly, J. W. (2005) *Chem. Biol.* **12**, 1235–1244